ELSEVIER

International Journal of Heat and Fluid Flow 23 (2002) 690–699

International Journal of HEAT AND FLUID FLOW

www.elsevier.com/locate/ijhff

Controlled transients of flow reattachment over stalled airfoils

Michael Amitay [a,*], Ari Glezer [b]

[a] ATAS Laboratory, Georgia Tech Research Institute, Atlanta, GA, USA
[b] School of Mechanical Engineering, Georgia Institute of Technology, Atlanta, GA, USA

Abstract

The flow transients associated with controlled reattachment and separation of the flow over a stalled airfoil are investigated in wind tunnel experiments. Control is effected using surface-mounted synthetic jet actuators that are typically operated at frequencies, which are at least an order of magnitude higher than the characteristic shedding frequency of the airfoil. While at these actuation frequencies the circulation (and hence the lift) of the attached flow is nominally time invariant, actuation at lower frequencies that are commensurate with the shedding frequency results in a Coanda-like attachment of the separated shear layer, organized vortex shedding and substantial oscillation of the circulation. The transients associated with flow reattachment and separation are investigated using amplitude modulation of the actuation waveform. Phase-locked measurements of the velocity field in the near wake of the airfoil and corresponding flow visualizations show that the transients that are associated with the onset of reattachment and separation are accompanied by the shedding of large-scale vortical structures and oscillations of the circulation. Pulsed modulated actuation of the actuation waveform is used to capture these transient effects and augment the increase in lift that is obtained by conventional time-harmonic actuation.

Keywords: Synthetic jets; Controlled reattachment and separation; Actuation frequency; Flow transients

1. Introduction

Active manipulation of separated flows over lifting surfaces at moderate and high angles of attack to achieve complete or partial flow reattachment with the objective of improving the aerodynamic performance and extending the flight envelope has been the focus of a number of investigations since the early 1980s. Coanda-like reattachment is normally effected by exploiting the receptivity of the separating shear layer to external excitation which affects the evolution of the ensuing vortical structures and their interactions with the flow boundary. Active flow control schemes that rely on the instability of the separating shear layer was demonstrated in a number of earlier investigations of separated flow (e.g., Ahuja and Burrin, 1984; Huang et al., 1987; Hsiao et al., 1990; Williams et al., 1991; Seifert et al., 1996).

Separation control by means of internal acoustic excitation (e.g., Huang et al., 1987) has typically employs an acoustically driven cavity within the airfoil in which (normally time harmonic) acoustic excitation is applied through a spanwise slot upstream of separation (typically near the leading edge of the airfoil). The work of Chang et al. (1992) confirmed earlier results of Hsiao et al. (1990), namely, that at low excitation levels, excitation at or near the unstable frequency of the separating shear layer ($St = f_{act}c/U_\infty = 2$, where f_{act} is the actuation frequency, c is the chord and U_∞ is the free stream velocity) can lead to a 50% increase in post-stall lift. Similar approach for the coupling of internal forcing to the predominant instabilities of the separating shear layer was also employed in the experiments of Wygnanski and Seifert (1994) and Seifert et al. (1996). These authors used unsteady jet blowing over several airfoil models to achieve various degrees of separation control by employing dimensionless actuation frequencies $St \sim O(1)$ (instead of St, these authors chose to denote the dimensionless actuation frequency as F^+; in their work the characteristic length scale x_s is the streamwise extent of the separated flow domain). However, an

* Corresponding author.
E-mail addresses: michael.amitay@me.gatech.edu (M. Amitay), ari.glezer@me.gatech.edu (A. Glezer).

0142-727X/02/$ - see front matter
PII: S0142-727X(02)00165-0

important contribution of the work of Chang et al. (1992) was the demonstration that the application of acoustic excitation at levels that are somewhat higher than those of their baseline experiments resulted in effective control of separation over a broad range of excitation frequencies (up to $St = 20$) that far exceed the unstable frequency of the separating shear layer.

Smith et al. (1998) and Amitay et al. (2001) demonstrated the utility of synthetic (zero mass flux) jet actuators for the suppression of separation over an unconventional airfoil at moderate Reynolds numbers (up to 10^6) resulting in a dramatic increase in lift and decrease in pressure drag. The jets are typically operated at dimensionless frequencies that are an order of magnitude higher than the shedding frequency of the airfoil (i.e., $St \sim O(10)$) and because they are zero net mass flux in nature, their interaction with the crossflow leads to local modification of the apparent shape of the flow surface. Full or partial reattachment including the controlled formation of a closed separation bubble, can be controlled by the streamwise location and the strength of the jets. The excitation is effective over a broad streamwise domain that extends well upstream of where the flow separates in the absence of actuation and even downstream of the front stagnation point on the pressure side of the airfoil. Furthermore, the work of Amitay and Glezer (1999) showed that while the circulation of the attached flow when actuation is applied at $St \sim O(10)$ is nominally time invariant, the shedding of organized vortical structures when actuation is applied at $St \sim O(1)$ leads to a time-periodic variations in the circulation (and therefore in the lift).

The sensitivity of the attached flow (and the restored lift) to the excitation frequency is also demonstrated in the numerical simulation of Donovan et al. (1998) who investigated flow reattachment over a NACA 0012 airfoil using time-harmonic zero mass flux blowing at $St = 1$. These simulations showed a 20% post-stall increase in lift at $\alpha = 22°$. However, the reattachment was similar to a Coanda-like effect where the forced shear layer deflected towards the airfoil surface, and the time-periodic vortex shedding from the top surface of the airfoil, led to 20% oscillations in the lift coefficient. Similarly, the more recent numerical simulations of Wu et al. (1998) reaffirmed that a separated flow can be effectively manipulated by low-level periodic blowing/suction near the leading edge. The forcing modulates the evolution of vortical structures within the separated shear layer and promotes the formation of concentrated lifting vortices, which in turn interact with trailing-edge vortices and thereby alter the global stalled flow. In a certain range of post-stall angles of attack and actuation frequencies, the flow becomes periodic and is accompanied by a significant lift enhancement.

The present work builds on earlier results of Amitay and Glezer (1999, 2001, 2002) and focuses on the transients associated with flow reattachment and separation when actuation is applied at frequencies for which $St \sim O(1)$ and also $St \sim O(10)$ (Section 3). As shown in Section 4, the transients associated with flow reattachment and separation can exploited to achieve an improvement in the efficiency of the jet actuators by pulsed modulation of the excitation input.

2. Experimental setup

The experimental setup is described in detail in the earlier work of Amitay et al. (2001). The experiments are conducted in an open return, wind tunnel having a test section measuring 91 cm on the side. The airfoil model is comprised of an aluminum leading edge circular cylinder mounted within a fiberglass aerodynamic fairing that is based on a uniformly stretched NACA four-digit series symmetric airfoil. The 62.2 mm diameter cylinder spans the entire test section and can be rotated about its axis within the fairing and is tangent to the surface of the fairing at the apexes of its cross-stream edges (where the airfoils has its maximum thickness). The chord of the combined cylinder-fairing airfoil is 25.4 cm, its thickness to chord ratio is 24% and its angle of attack a can be independently varied between $-25°$ and $25°$.

The center section of the cylinder houses a pair of adjacent synthetic jet actuators each having a flush-mounted rectangular orifice (0.5 mm wide and 140 mm long). The orifices are collinear with respect to the axis of the cylinder along their long dimension, and separated by 2.5 mm. The actuator performance is measured using the momentum coefficient, $C_\mu = \bar{I}_j/\frac{1}{2}\rho_0 U_0^2 c$, where $\bar{I}_j$ is the jet time-averaged momentum flux per unit length during the outstroke (Smith and Glezer, 1998), ρ_0 and U_0 are the free stream density and velocity, respectively, and c is the chord.

The cylinder section of the airfoil is instrumented with 47 pressure taps that are located in the spanwise mid-plane and are equally spaced circumferentially around the cylinder. Similarly, the fairing is instrumented with 45 pressure taps along the top and bottom surfaces and at the same spanwise location as the taps on the cylinder. Cross-stream distributions of the streamwise and cross-stream velocity components are measured in the wake of the airfoil using x-configuration hot wire miniature sensors that are mounted on a computer-controlled traversing mechanism. In addition, the velocity and vorticity distributions in the cross-stream (x–y) plane, $z = 0$, above the airfoil (i.e., on the suction side) are measured using particle image velocimetry (PIV) using a 1008×1016 pixel CCD camera with a magnification of 53 μm/pixel (the nominal particle diameter is sub-pixel). Velocity vectors are computed on a 62×62 grid using a standard cross-correlation

technique. Each of the ensemble-averaged data maps consists of 150 realizations (image pairs).

3. Flow transients associated with reattachment and separation

The enhancement of the aerodynamic performance of the present airfoil using synthetic jet actuators is discussed in detail in earlier papers by Smith et al. (1998) and Amitay et al. (2001). These works show that the flow over the airfoil at post-stall angles of attack can be attached using actuation effected by synthetic jet actuators that are integrated into the surface of the airfoil. The actuation results in a substantial increase in the lift and concomitantly in reduced pressure drag. Furthermore, the modification of the aerodynamic forces on the airfoil is accompanied by substantial decease in the cross-stream width of the wake and in the evolution of the large-scale vortical structures.

In what follows, the dynamics of the reattachment and separation processes following an onset and termination of pulsed amplitude modulation of the actuator (control) input are presented for which the dimensionless frequency of the actuation signal is either $St \sim O(1)$ or O(10). The modulation is synchronized with the actuator's driving signal such that the leading edge of the modulating waveform coincides with a zero crossing of the actuator signal and continues for 0.5 s. Using x-wire anemometry, the transients of the flow resulting from the pulsed excitation is measured in detail across the near wake at $\hat{x} = x/c = 2$. The airfoil is placed at an angle of attack of 17.5°, the jets issue from the suction side of the airfoil at $\gamma = 60°$ where the corresponding downstream distance from the leading edge is $\hat{x} = 0.062$ (γ is the angle between the jets' centerline and the free stream), the momentum coefficient is 3.5×10^{-3}, the free stream velocity is 18.5 m/s, and $Re_C = 310{,}000$.

The phase-averaged cross-stream distributions of the dimensionless spanwise vorticity is computed from the streamwise and cross-stream velocity distributions (not shown) and are shown in Fig. 1a and b for $St = 10$ and 0.95, respectively (the up and down arrows denote the times where the control is turned on and off, respectively). Note that $\hat{y}$ corresponds to the leading edge of the airfoil (cf. Amitay and Glezer, 2001) and U_∞, T (the actuation period), and c are used to render all variables dimensionless. When the flow is separated (i.e., before

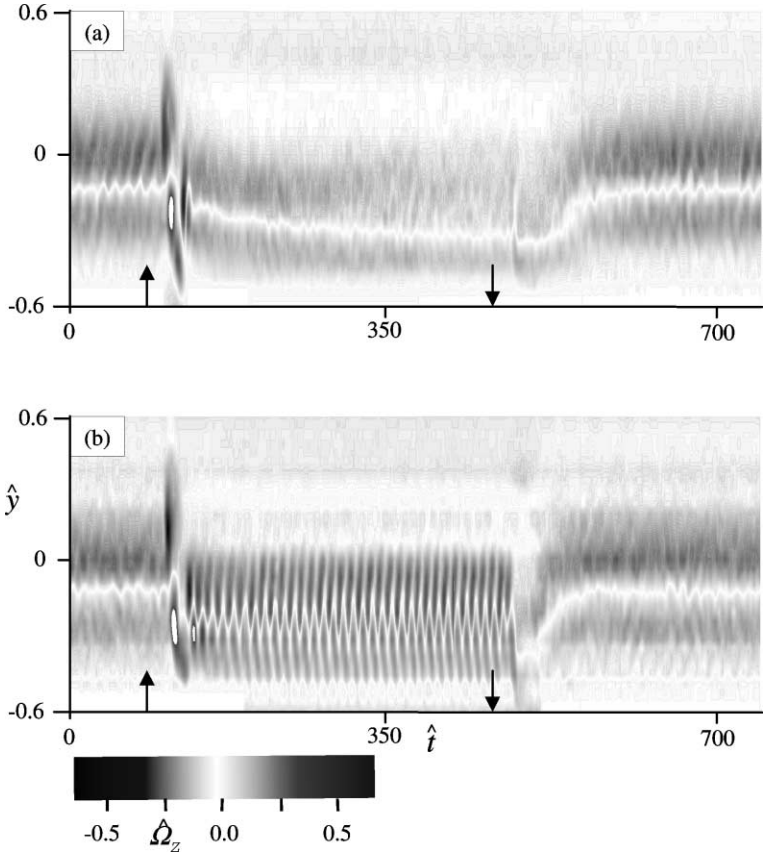

Fig. 1. Phase-averaged black and white raster plot of the cross-stream distribution of the spanwise vorticity measured at $x/c = 2$; (a) $St = 10$ and (b) $St = 0.95$.

and after the pulse modulated excitation is applied), the vorticity distribution in the wake is comprised of a train of vortical structures of alternating sign (clockwise vorticity is taken to be negative) having a nominal passage frequency of 50 Hz. Nevertheless, the total vorticity flux across the wake during one period of the (baseline) shedding frequency is approximately zero.

As was shown by Smith et al. (1998), the actuation leads to flow reattachment and the establishment of a higher (positive) lift force on the airfoil, which must be accompanied by a change in the vorticity flux and a net increase in circulation associated with positive (counter-clockwise) vorticity. However, following the reattachment, a strong clockwise vortex indicating *a reduction in lift* is initially advected past the measurement station. This vortex is inherent of a separated flow and it is associated with the negative "trapped" vorticity that must shed off the airfoil. The shedding of the negative vorticity is followed closely by a stronger counter-clockwise vortex indicating the reestablishment of lift ("starting vortex"). These two large vortices are followed by a series of smaller vortices of alternating signs and diminishing strength. It is remarkable that the initial transient following the application of the high-frequency pulse-modulated control (Fig. 1a) are very similar to that of the low-frequency actuation (Fig. 1b). However, in contrast to the reattachment at the higher reduced frequency in which the shedding of organized vortical structures appears to subside following the transient (for $\hat{t} > 300$, Fig. 1a), the reattachment at a reduced frequency of order one appears to be accompanied by the coherent shedding of a train of strong vortices at the actuation frequency.

When the control is turned off, the flow separates again and the airfoil loses its lift. This reduction in lift is accompanied by a decrease in circulation and the shedding of negative (clockwise) vorticity. However, immediately following the termination of the control, a counter-clockwise vortex indicating *a momentary increase in lift* is advected past the measurement station before the separated vorticity field is established. These flow transients are similar at both actuation frequencies suggesting that the separation process is similar.

These data suggest that when the flow is actuated at a low reduced frequency, which is of the same order of the natural shedding frequency to which the separated flow is inherently receptive, the control input is amplified and the reattachment is manifested by the passage of shear layer vortices along the surface of the airfoil. However, when the actuation frequency is high enough, the interaction of the jets with the flow occurs at a smaller length scale, which leads to local modification of the apparent shape of the airfoil, and suppresses the shedding of large-scale vortices (for more details of the interaction of a synthetic jet with a crossflow see Honohan et al., 2000).

As noted by Amitay et al. (1999), the time rate of change of the circulation is given by the phase-averaged vorticity flux

$$\frac{\mathrm{d}\langle\hat{\Gamma}\rangle}{\mathrm{d}\hat{t}} = \int_{-\infty}^{\infty} \langle\hat{U}\rangle\langle\hat{\Omega}_z\rangle \,\mathrm{d}\hat{y}. \tag{1}$$

Here, $\langle\hat{\Gamma}\rangle$, $\langle\hat{U}\rangle$, $\langle\hat{\Omega}_z\rangle$ and $\hat{t}$ are the normalized phase-averaged circulation, streamwise velocity, spanwise vorticity and time, respectively. By integrating the vorticity flux, $\mathrm{d}\langle\hat{\Gamma}\rangle/\mathrm{d}\hat{t}$, the phase-averaged increment (relative to the baseline flow) of the circulation, $-\Delta\langle\hat{\Gamma}\rangle$, is estimated and shown in Fig. 2 ($St = 0.95$ and 10 are shown using solid and dashed curves, respectively). Note that the integration does not account for contributions of the fluctuating components, and it is assumed that because the measurement station is located only one chord-length downstream of the trailing edge of the airfoil, which is shorter than the wavelength of the shedding frequency, the interaction between successive vortices within this domain is minimal.

When the flow reattachment begins, $-\Delta\langle\hat{\Gamma}\rangle$ exhibits a similar transient at both control frequencies. The incremental change in the circulation with respect to the baseline flow $-\Delta\langle\hat{\Gamma}\rangle$ initially diminishes to a value of -0.6 (resulting in a momentary decrease in the lift coefficient) and then recovers to a value of 0.33 and 0.43 (for $St = 0.95$ and 10, respectively) with the shedding of the second counter-clockwise vortex. It appears that the shedding of the starting vortex causes partial trailing edge separation, which is manifested by the shedding of another (weaker) clockwise vortex followed by a train of vortices of alternating signs (see cartoon). The circulation (and lift coefficient) ultimately converges to

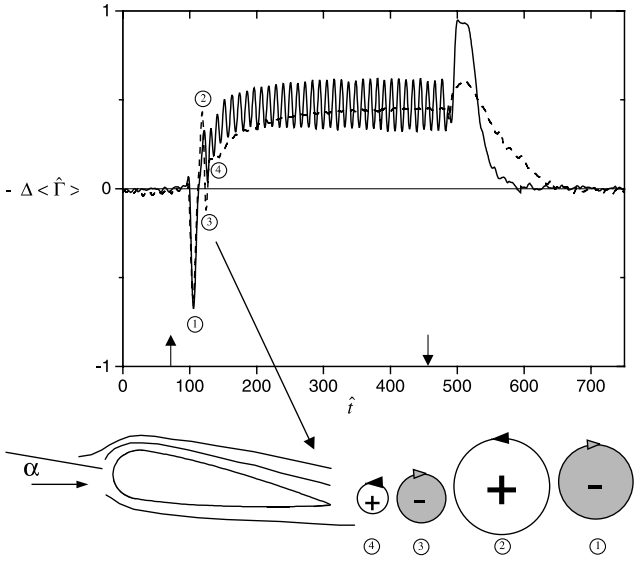

Fig. 2. Phase-averaged circulation increment for $\alpha = 17.5°$ and $\gamma = 60°$. $St = 0.95$ (—), and 10 (- - -).

its attached value, which is in good agreement with the lift coefficient obtained from previous pressure measurements (Smith et al., 1998). However, while for high frequency actuation the circulation ultimately reaches a steady level, low-frequency actuation results in oscillations of $-\Delta\langle\hat{\Gamma}\rangle$ at the actuation frequency with peak-to-peak fluctuations of up to 55% of the mean level for the attached flow.

When the control is turned off the circulation initially increases before settling to the baseline-stalled level, which is similar to the transient variation of lift on a pitching airfoil during dynamic stall.

The flow mechanisms associated with the controlled reattachment process (at $St = 10$) are demonstrated in a sequence of smoke visualization images in Fig. 3a–f (the separated flow, in the absence of control, is shown for reference in Fig. 3a). The smoke is injected in a sheet at the center span and is illuminated using a pulsed laser. At $\hat{t} = 8$ after the control is activated (Fig. 3b) a vortex with a negative vorticity, which is associated with the shedding of the trapped vorticity of the separated flow, is formed near the leading edge. At $\hat{t} = 18$ (Fig. 3c), this vortex has grown in size and is advected downstream. Note the beginning of the formation of a second vortex with a negative vorticity near the leading edge. As time progresses these two vortices continue to advect towards the trailing edge while increasing in size (by the time the first vortex reaches the trailing edge its size is more than half of the airfoil's chord, Fig. 3d). At $\hat{t} = 33$ (Fig. 3e) a third vortex is formed, however, this vortex resides near the surface of the airfoil and does not increase in size as the first two vortices. Following the transient ($\hat{t} = 125$, Fig. 3f) the flow is completely attached to the surface of the airfoil and there is no evidence of vortical structures. Note that the vortices with a positive vorticity that contribute to the establishment of a positive lift are not present in these flow visualization images because they are shed from the trailing edge off the window used for the flow visualization.

Note that the effects of the jet location, the momentum coefficient, the Reynolds number and the actuation frequency on the global behavior of the flow around the airfoil is discussed in detail in the earlier papers by Smith et al. (1998) and Amitay and Glezer (2002).

4. Aerodynamic performance enhancement using pulse-modulated actuation

The flow transients associated with the controlled reattachment and separation processes that are described in Section 3 are exploited to further enhance the effectiveness of the jet actuators. Pulse-modulation of the actuation input, which may be useful in situation when either the streamwise placement or the strength of the jet actuators are sub-optimal is demonstrated by placing the jet actuator at $\gamma = 42°$, where as shown in the earlier work of Smith et al. (1998), C_μ yields some measure of proportional control of the lift coefficient. The effect of C_μ on the distribution of the pressure coefficient around the airfoil (at $St = 10$) is shown in Fig. 4 for $C_\mu = 3.7 \times 10^{-3}$ and 4.6×10^{-3} (open and solid symbols, respectively; the pressure distribution in the absence of control is shown using a solid curve). It is evident that when $C_\mu = 4.6 \times 10^{-3}$, the flow is fully attached ($C_L = 0.8$) and a strong low-pressure region is present near the leading edge on the suction side of the airfoil followed by a rapid pressure recovery towards the trailing edge. However, a relatively small (18%) reduction of the momentum coefficient to $C_\mu = 3.75 \times 10^{-3}$,

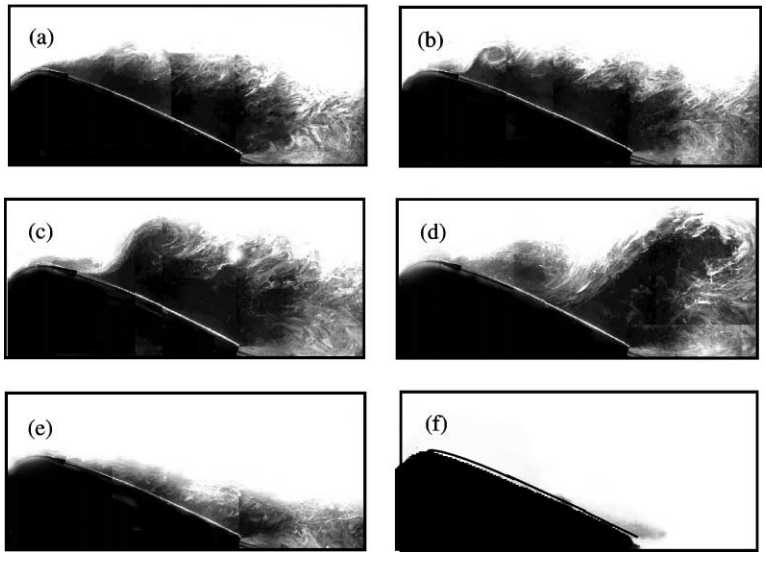

Fig. 3. Phase-averaged images during the reattachment process for $\alpha = 17.5°$, $\gamma = 60°$, and $St = 10$. $\hat{t} = 0$ (a), 8 (b), 18 (c), 24 (d), 33 (e) and 125 (f).

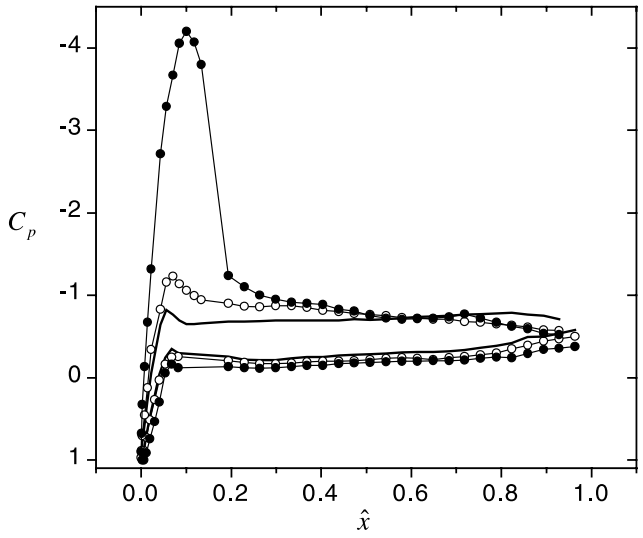

Fig. 4. Pressure coefficient distributions around the airfoil. (•) $C_\mu = 4.6 \times 10^{-3}$, (○) $C_\mu = 3.75 \times 10^{-3}$, and (—) baseline.

results in a partially reattached flow and a substantial degradation of the lift coefficient to $C_L = 0.4$. The pressure distribution exhibits a much smaller suction peak near the leading edge followed by a separation bubble that extends throughout most of the upper surface of the airfoil.

By exploiting the flow transients that are associated with the onset and removal of the actuation, the performance of the actuators at reduced levels of momentum coefficient, can be substantially enhanced by pulse modulation of their resonance waveform (nominally at $St = 10$). While the period t' and duty cycle $\tilde{d}$ of the modulating pulse train can independently varied, in what follows $\tilde{d} = 0.25$ and the modulating frequency $\hat{f} = 1/t'$ is varied between 0.27 and 5.0.

The long-term variation of the phase-averaged (i.e., relative to the modulating wavetrain) circulation with $\hat{f}$ following the decay of the initial transients is shown in Fig. 5a–d for $\hat{f} = 0.27$, 1.1, 3.3 and 5.0, respectively (the time trace corresponding to the unmodulated actuation is shown for reference in each plot using symbols). The modulation frequency $\hat{f} = 0.27$ (Fig. 5a) corresponds to the "natural" passage frequency of the vortices during the initial (transient) stages of the reattachment process (Fig. 2). The resulting quasi-steady circulation exhibits oscillations that are similar in magnitude and duration to the transient stages of the reattachment with shedding of similar vortical structures. The phase of each pulse of the modulating wave train is timed so that it retriggers reattachment before the flow separates again. This phase is evidently a bit off, because the circulation apparently exhibits low-frequency variations (having a period of the order of $60T$). When $\hat{f}$ is increased to 1.1 the elapsed time between pulses within the modulating wave train is decreased (Fig. 5b) and the large oscillations in the circulation are substantially attenuated. This suggests that the modulating pulses are timed to prevent continuous shedding of large vortical structures and the corresponding variations in circulation. The recovery of an asymptotic circulation of approximately $-\langle \Delta\hat{\Gamma} \rangle = 0.45$ also suggests that the actuation allows the accumulation and maintenance of (clockwise) vorticity on the suction side of the airfoil even though the reattachment is unsteady and the circulation oscillates with peak-to-peak variations of 42% of its asymptotic mean level.

Further increase in $\hat{f}$ to 3.3 (Fig. 5c) results in a circulation that is similar to the magnitude of the

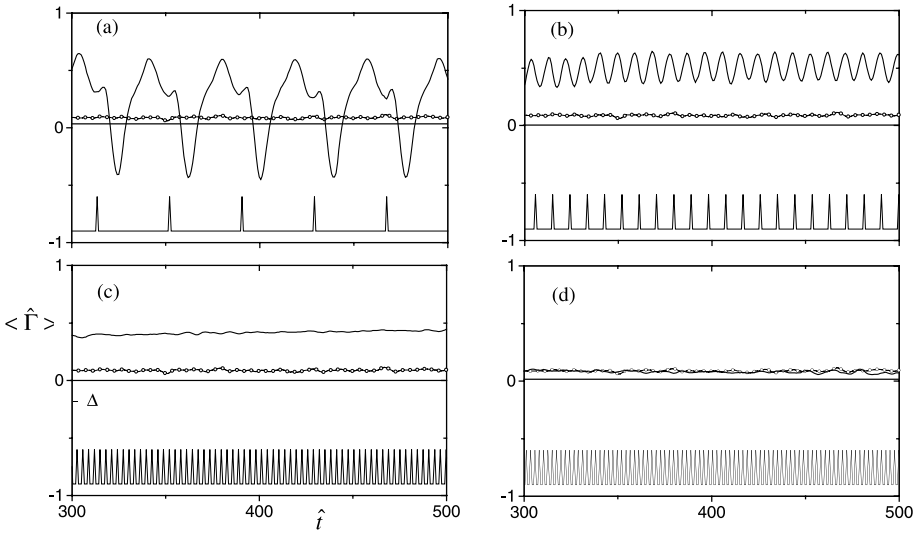

Fig. 5. Long-term variation of the phase-averaged circulation increment for $\alpha = 17.5°$ and $\gamma = 42°$. $\hat{f} = 0.27$ (a), 1.1 (b), 3.3 (c) and 5.0 (d).

piecewise-averaged circulation in Fig. 5b ($\hat{f} = 1.1$). However, the absence of oscillations at the modulating frequency indicates optimal timing between the modulating pulses. It is remarkable that pulse modulation yields an increase of ~400% in the lift coefficient (when it reaches steady state) compared to continuous high-frequency actuation but at 25% of the jet momentum coefficient. Finally, when the modulating frequency is further increased to $\hat{f} = 5$ (Fig. 5d), the time between successive pulses of the modulating wave train is apparently too short to capture the unsteady vortical structures. The effectiveness of the modulation is minimal and the circulation returns to the same levels obtained with a continuous pulse train.

Given these results, it might be argued that a lift coefficient increment similar to that of Fig. 5c may be obtained by simply operating the jet actuators time harmonically at $St = \hat{f}$ thus bypassing the need for pulse modulation altogether. This argument is tested by comparing the effect of both actuation approaches namely, time harmonic excitation at $St = 3.3$ and pulse modulation at $\hat{f} = 3.3$ while maintaining the same jet momentum coefficient. Time traces of the normalized circulation for both cases are shown in Fig. 6 (time harmonic actuation is plotted using symbols). Also shown are the input waveforms that lead to identical C_μ over one period of the actuation. These data clearly show that time harmonic actuation does not yield the same levels of lift coefficient as pulse modulated actuation.

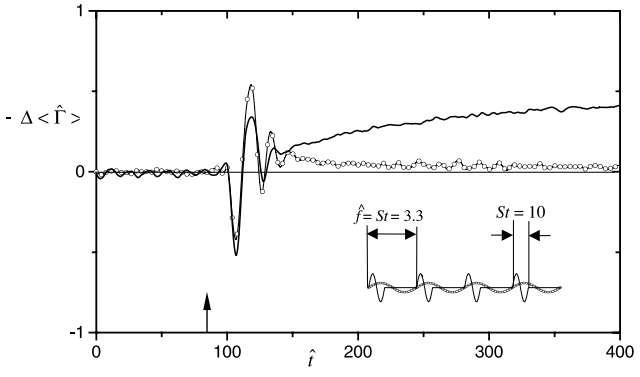

Fig. 6. Phase-averaged circulation increment for $\alpha = 17.5°$ and $\gamma = 42°$. (○) Continuous periodic actuation and (—) pulsed reattachment technique.

To further demonstrate the effectiveness of the pulse reattachment technique the flow field above the airfoil is computed using a sequence of PIV images taken in the x–y plane ($z = 0$) over the upper surface of the airfoil. Each image is comprised of three partially overlapping frames measuring 10×10 cm^2. The data are acquired at $\alpha = 20°$, $Re_c = 310,000$, $\gamma = 45°$, and $C_\mu = 4.5 \times 10^{-3}$. Each image is comprised of three partially overlapping frames each consisting of 150 realization pairs. Cross-stream maps of time-averaged velocity vectors are shown in Fig. 7a–d. In the absence of control (Fig. 7a), the separated flow exhibits a large recirculating flow domain above the entire upper surface of the airfoil. At this low level of C_μ, unmodulated actuation at $St = 10$ (Fig. 7b) leads to a slight downstream migration (to $\hat{x} \approx 0.3$) of the point of separation and the flow is completely separated thereafter.

When the flow is actuated using pulse modulated actuation at $\hat{f} = 1.1$ of an $St = O(10)$ carrier (Fig. 7c), the flow is attached over most of the surface of the airfoil. It is interesting to note that for $\hat{x} > 0.7$, the boundary layer of the attached flow becomes noticeably thicker presumably as a result of a sub-optimal pressure recovery. The vector image suggests that the flow may be separated just upstream of the trailing edge of the

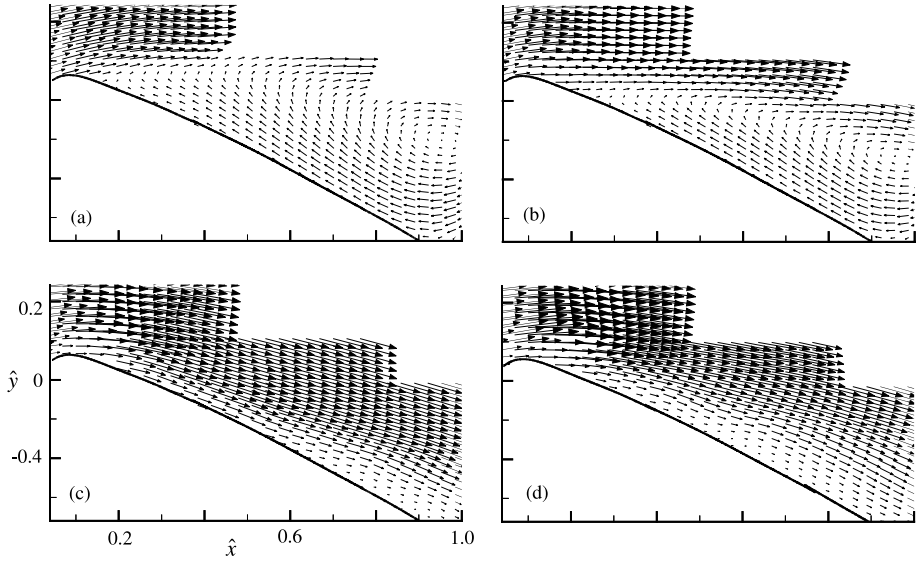

Fig. 7. Time-averaged velocity vector fields for $\alpha = 20°$ and $\gamma = 45°$. Baseline (a), $St = 10$ (b), and $\hat{f} = 1.1$ (c), and $St = 1.1$ (d).

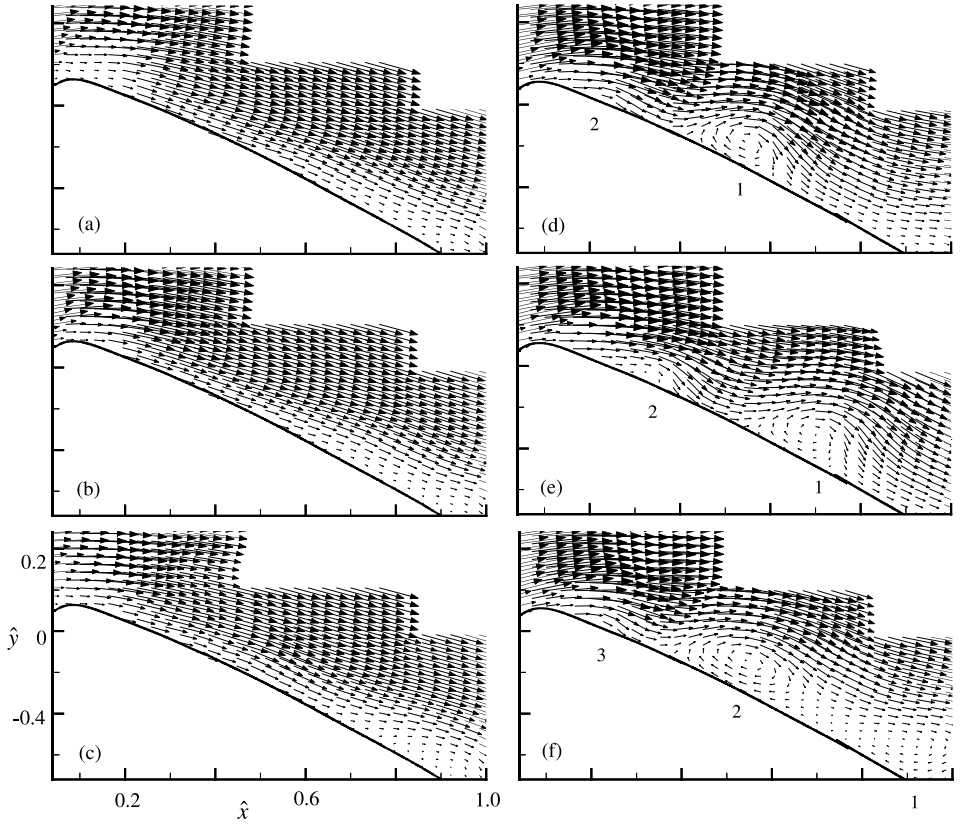

Fig. 8. Velocity vector fields for $\alpha = 20°$, $\gamma = 45°$, $\hat{f} = 1.1$ (a,b,c) and $St = 1.1$ (d,e,f); at different phases.

airfoil. A comparison of this vector map with the corresponding map for unmodulated actuation at $St = 1.1$ (Fig. 7d) shows that the unmodulated actuation results in thickening of the wall layer that commences much farther upstream (i.e., $\hat{x} > 0.2$).

Phase-averaged velocity vector maps corresponding to the pulse modulated and unmodulated actuation are shown in Fig. 8a–f, respectively, at three phases. While the phase-averaged vector maps for actuation at $\hat{f} = 1.1$ (Fig. 8a–c) exhibits an attached flow, where the flow fields at the three phases are very similar (there is a slight difference near the trailing edge), unmodulated actuation at $St = 1.1$ (Fig. 8d–f) results in the rollup and advection of coherent vortical structures at the actuation frequency having a nominal characteristic wavelength of $0.4c$.

Distributions of the pressure coefficient around the airfoil for $St = 1.1$ and $\hat{f} = 1.1$ are shown in Fig. 9. The pressure distribution for the baseline stalled flow (solid line) is also shown for reference. Actuation with the pulse modulation ($\hat{f} = 1.1$, solid circles) leads to a large suction peak around $\hat{x} = 0.1$ with a pressure recovery downstream of the suction peak, suggesting that the flow is fully attached to the surface of the airfoil. The corresponding distributions of pressure coefficient for $St = 1.1$ with $C_\mu = 3.5 \times 10^{-3}$ (an order of magnitude larger than for actuation using pulse reattachment) results in a similar suction peak. However, unlike the pulse modulation actuation the pressure recovery downstream of the suction peak appears to be less rapid with a separation bubble near the trailing edge. A more accurate comparison is to compare the effect of both actuation approaches namely, time harmonic excitation at $St = 1.1$ and pulse modulation at $\hat{f} = 1.1$ while maintaining the same jet momentum coefficient. Actuation at

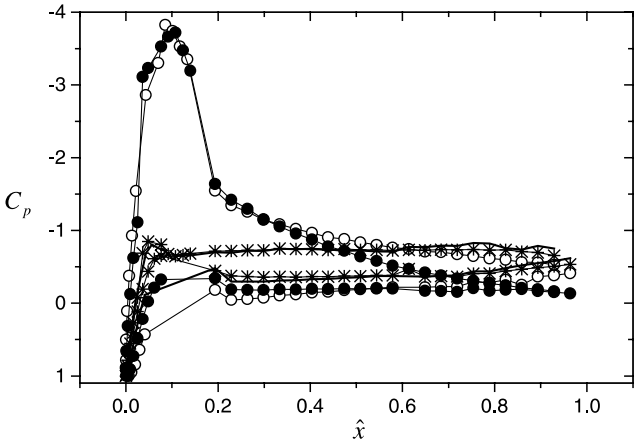

Fig. 9. Pressure coefficient distributions around the airfoil, $\alpha = 20°$, $\gamma = 45°$. $\hat{f} = 1.1$, $C_\mu = 5.4 \times 10^{-4}$ (●); $St = 1.1$, $C_\mu = 5.4 \times 10^{-3}$ (○); $St = 1.1$, $C_\mu = 5.4 \times 10^{-4}$ (*) and baseline (—).

$St = 1.1$ with $C_\mu = 3.5 \times 10^{-4}$ (star symbols) yields a negligible effect on the pressure distribution around the airfoil, suggesting that by simply operating the jet actuators time harmonically at $St = \hat{f}$ (thus bypassing the need for pulse modulation altogether) is not sufficient to obtain the same lift coefficient increment.

5. Conclusions

The present paper reports a wind tunnel investigation of the manipulation of the global aerodynamic forces on a thick airfoil using surface-mounted synthetic jet actuators. The response of the flow over the airfoil to time-modulated control input is measured in the cross-stream plane of the airfoil wake using phase-locked two-component hot-wire anemometry, while the flow field over the airfoil is measured using phased-locked PIV. The effect of the actuation is investigated at two ranges of jet actuation frequencies ($St \sim O(1)$ and $O(10)$).

Flow reattachment over the stalled airfoil begins with the advection of a strong clockwise vortex (trapped vorticity) past the measurement station indicating a reduction in lift that is followed closely by a stronger counter-clockwise vortex indicating the reestablishment of lift. For the high-frequency actuation the reduced wake of the attached flow ultimately reaches a quasi-steady state of symmetric vorticity distribution. In contrast to the reattachment at $St \sim O(10)$, when the reduced actuation frequency is O(1), the reattachment is followed by the coherent shedding of a train of strong vortices at the actuation frequency. When the flow reattachment begins, the phase-averaged change in circulation with respect to the baseline flow, $-\langle\Delta\hat{\Gamma}\rangle$, exhibits a similar transient at both control frequencies. However, while for high frequency forcing the circulation (and thus the lift coefficient) ultimately reaches a steady level, low-frequency actuation results in oscillations of $\langle\Delta\hat{\Gamma}\rangle$ (and C_L) at the actuation frequency with peak-to-peak fluctuations of up to 55% of the mean level for the attached flow.

The flow mechanisms associated with the reattachment process are demonstrated in a sequence of smoke visualization images. Following the activation of the control a vortex with a negative vorticity is formed near the leading edge. This vortex is due to the negative vorticity associated with the separated flow. The vortex is advected downstream and increases in size and a second vortex is formed near the leading edge. As time progresses these two vortices continue to increase in size, and near the trailing edge the size of the first vortex is more than half of the airfoil's chord. Following the transient, the flow is completely attached to the surface of the airfoil and there is no evidence of vortical structures.

The second part of the paper describes a new actuation technique that is used to achieve an improvement in the efficiency of the jet actuators by using pulse modulated excitation input. Pulse modulation frequency of successive bursts of the driving signal helps to "capture" the vorticity produced during the initial stages of the separation process on the suction side of the airfoil and thus to increase the lift force. The actuator resonance waveform (nominally at $St = 10$) is pulse modulated such that the period and duty cycle of the modulating pulse train are independently controlled. The duty cycle was restricted to 25% and the modulating frequency $\hat{f}$ was varied between 0.27 and 5.0. When the modulation frequency is $\hat{f} = 0.27$ (corresponds to the natural passage frequency of the vortices during the initial transient stages of the reattachment process), the circulation exhibits oscillations that are similar to the transient stages of the reattachment with shedding of similar vortical structures. When $\hat{f}$ is increased to 1.1 the large oscillations in the circulation are substantially attenuated. Further increase in $\hat{f}$ to 3.3 results in a circulation (and consequently lift coefficient) that is similar to the magnitude of the piecewise-averaged circulation at $\hat{f} = 1.1$ but the absence of oscillations. When the modulating frequency is increased further to $\hat{f} = 5$, the effectiveness of the modulation is minimal and the lift coefficient returns to the same levels obtained with a continuous (high frequency) pulse train.

Given these results, it might be argued that a lift coefficient increment similar to $\hat{f} = 3.3$ may be obtained by simply operating the jet actuators time harmonically at $St = \hat{f}$ thus bypassing the need for pulse modulation altogether. This argument was tested by comparing the effect of both actuation approaches namely, time harmonic excitation at $St = 3.3$ and pulse modulation at $\hat{f} = 3.3$ while maintaining the same jet momentum coefficient. This comparison shows that time harmonic actuation does not yield the same levels of lift coefficient as pulse modulated excitation.

Acknowledgements

This work was supported in part by AFOSR (monitored by Dr. T. Beutner), DARPA, and by The Boeing Company, St. Louis. The authors gratefully acknowledge contributions by Drs. V. Kibens, M. Lal and D.E. Parekh.

References

Ahuja, K.K., Burrin, R.H., 1984. Control of flow separation by sound. AIAA Paper, 84–2298.

Amitay, M., Glezer, A., 1999. Aerodynamic flow control of a thick airfoil using the synthetic jet actuators. In: Proceedings of the 3rd ASME/JSME Joint Fluids Engineering Conference, San Francisco, California.

Amitay, M. and Glezer, A., 2001. The dynamics of controlled flow reattachment and separation over stalled airfoils. In: 2nd International Symposium on Turbulence and Shear Flow Phenomena, Stockholm, Sweden.

Amitay, M. and Glezer, A., 2002. Role of actuation frequency in controlled flow reattachment over a stalled airfoil. AIAA Journal 40, 209–216.

Amitay, M., Kibens, V., Parekh, D.E., Glezer, A., 1999. Flow reattachment dynamics over a thick airfoil controlled by synthetic jet actuators. AIAA Paper 99-1001.

Amitay, M., Smith, D.R., Kibens, V., Parekh, D.E., Glezer, A., 2001. Aerodynamic flow control over an unconventional airfoil using synthetic jet actuators. AIAA Journal 39 (3), 361–370.

Chang, R.C., Hsiao, F.-B., Shyu, R.-N., 1992. Forcing level effects of internal acoustic excitation on the improvement of airfoil performance. Journal of Aircraft 29 (5), 823–829.

Donovan, J.F., Kral, L.D., Cary, A.W., 1998. Active flow control applied to an airfoil. AIAA Paper, 98–0210.

Honohan, A.M., Amitay, M., Glezer, A., 2000. Aerodynamic control using synthetic jets. AIAA Paper 2000-2401.

Hsiao, F.-B., Liu, C.-F., Shyu, J.-Y., 1990. Control of wall-separated flow by internal acoustic excitation. AIAA Journal 28 (8), 1440–1446.

Huang, L.S., Maestrello, L., Bryant, T.D., 1987. Separation control over an airfoil at high angles of attack by sound emanating from the surface. AIAA Paper 87-1261.

Seifert, A., Darabi, A., Wygnanski, I., 1996. Delay of airfoil stall by periodic excitation. Journal of Aircraft 33 (4), 691–698.

Smith, B.L., Glezer, A., 1998. The formation and evolution of synthetic jets. Physics of Fluids 31, 2281–2297.

Smith, D.R., Amitay, M., Kiben, K., Parekh, D.E., Glezer, A., 1998. Modification of lifting body aerodynamics using synthetic jet actuators. AIAA Paper 98-0209.

Williams, D. R., Acharya, M., Bernhardt, J. and Yang, P.-M., 1991. The mechanism of flow control on a cylinder with the unsteady bleed technique. AIAA Paper 91-0039.

Wu, J.-Z., Lu, X.-Y., Denny, A.G., Fan, M., Wu, J.-M., 1998. Post-stall control on an airfoil by local unsteady forcing. J. of Fluid Mech. 371, 21–58.

Wygnanski, I., Seifert, A., 1994. The control of separation by periodic oscillations. AIAA Paper 94-2608.